23. Basu, P.; Panayotov, D.; Yates Jr., J. T. *J. Phys. Chem.* **1987,** *91*, 3133.
24. Paul, D. K.; Yates Jr., J. T. *J. Phys. Chem.* **1991,** *95*, 1699.
25. Paul, D. K.; Ballinger, T. H.; Yates Jr., J. T. *J. Phys. Chem.* **1990,** *94*, 4617.
26. Mizushima, T.; Tohji, K.; Udagawa, Y. *J. Phys. Chem.* **1990,** *94*, 4980.
27. Solymosi, F.; Rasko, J. *J. Catal.* **1989,** *15*, 107.
28. Anderson, S. L.; Mizushima, T.; Udagawa, Y. *J. Phys. Chem.* **1991,** *95*, 6603.
29. Boudart, M.; Hwang, H. *J. Catal.* **1975,** *39*, 44.
30. Slichter, C. P. *Principles of Magnetic Resonance* 3rd Ed.; Springer-Verlag: Berlin, 1990.
31. Stejskal, E. O.; Schaefer, J. *J. Magn. Reson.* **1974,** *14*, 160.
32. Homans, S. W. *A Dictionary of Concepts in NMR*; Oxford University Press: New York, 1989.
33. Shore, E. S.; Ansermet, J.-P.; Slichter, P. C. *Phys. Rev. Lett.* **1987,** *58*, 953.
34. Mehring, M. *Principles of High Resolution in NMR in Solids* 2nd Ed.; Springer-Verlag: Berlin, 1983.
35. Sheu, L.-L.; Karpinksi, Z.; S achtler, M. H. *J. Phys. Chem.* **1989,** *93*, 4890.

Structural and Optical Properties of the $(C_nH_{2n+1}NH_3)_2SnCl_4$ (n=2, 4, 6, 8, and 10) System

Ri-Zhu Yin and Chul Hyun Yo*

Department of Chemistry, Yonsei University, Seoul 120-749, Korea
Received March 13, 1998

K_2NiF_4-type layered compounds of the $(C_nH_{2n+1}NH_3)_2SnCl_4$ (n=2, 4, 6, 8, and 10) system have been synthesized from a stoichiometric mixture of $SnCl_2$ and alkyl ammonium salt using a low temperature solution technique under the inert atmosphere condition. Their crystal structures are assigned to the orthorhombic system by X-ray powder diffraction analysis. The a and b cell parameters show small changes. However, the c parameter is varied significantly according to the increment of alkyl chains of the organic layer which is located between inorganic layers in the compounds. The conformational phase transitions of the compounds are studied by the DSC in the temperature range of 300 to 500 K. FT-IR and Raman spectra are analyzed in the ranges of 1300 to 4000 cm^{-1} and of 50 to 360 cm^{-1} with Ar-laser (λ=514.5 nm) excitation, respectively. Photoluminescence phenomena are observed for some compounds. The bond-length of Sn-Cl is determined by the EXAFS spectroscopic analysis.

Introduction

Recently, much attention has been focused on organic-inorganic layered perovskites due to the tuneability of their special structural features and interesting physical properties. In the K_2NiF_4 type families of the formula $(C_nH_{2n+1}NH_3)_2$-MX_4 (where M is a divalent metal, and X is halogen), the MX_4^{2-} layers are sandwiched between organic barrier layers consisting of alkylammonium chains. As shown in Figure 1, the inorganic layers are built up from corner sharing halogen octahedra with an M^{2+} ion in the centers. The cavities between the octahedra are occupied by the RNH_3^+ polar head.[1]

Since the dielectric constant of barrier layer is much smaller than that of perovskite layers, the above compounds are known as natural quantum-well structures and fabricated to obtain devices with the required performance such as an electroluminescent device. Another benefit of the quantum-well structure is the ability to provide stages to study some basic phenomena such as the transport mechanism or the control of spontaneous emission by designing appropriate structures.[2]

In low dimensional semiconductor quantum-well structures, the Coulomb interaction between an electron and a hole is enhanced by the quantum confinement effect.[3] The exciton binding energy in the two-dimensional structure is known to be four times larger than that in the bulk structures.[4] The quantum-well materials are applicable for use in non-linear optical, photoluminescent and electro-luminescent devices due to excitonic effects.

The mechanism of the structural phase transition has been divided into two main classes.[5] One is an order-disorder transition of the rigid alkylammonium chains. The other is conformational transitions leading to a partial "melting" of the hydrocarbon atom with large enough $n \geq 4$. Some of them show one main and other minor transitions. The main transition with the largest enthalpy variation is often referred to as the "melting" of the alkylchain and the minor transition has been assigned to the onset of reorientational motions of the NH_3^+ head group.[6]

A heterostructure electroluminescent device using $(C_6H_5C_2H_4NH_3)_2PbI_4$ as an emitter material has been demonstrated. The device produces highly intense green electroluminescence of the luminosity more than 10,000 cd/

*Author to whom correspondence should be addressed.

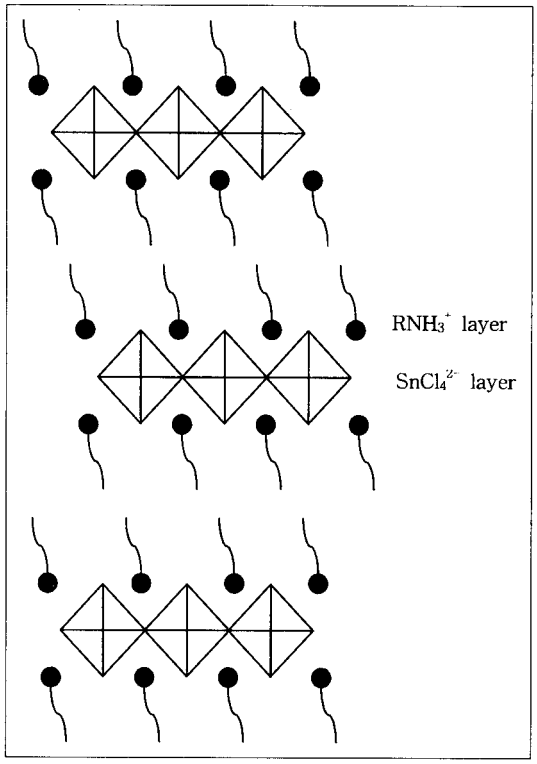

Figure 1. Schematic structure of the bilayer $(RNH_3)_2SnCl_4$ compounds

m^2 at liquid nitrogen temperature with a current density of 2 A/cm^2 and an operating voltage of 24 V.[7] The compounds form stable exciton with a large binding energy even at room temperature owing to their low-dimensional semiconductor nature. Thus many compounds of the layered perovskite family exhibit photoluminescence from the exciton band. The flexibility of the material design makes tuneable exciton emission which is desired to apply to the device.

In the present study, the structural and optical properties for the compounds of $(C_nH_{2n+1}NH_3)_2SnCl_4$ (n=2, 4, 6, 8, and 10) have been investigated. The compounds are synthesized by a low temperature solution technique. The structures have been identified by X-ray diffraction, extended X-ray absorption fine structure (EXAFS), FT-IR, and Raman spectroscopies. The phase transitions are determined by differential scanning calorimetry (DSC), and then photoluminescence (PL) phenomena have also been discussed.

Experimental

Synthesis of the $(C_nH_{2n+1}NH_3)_2SnCl_4$ (n=2, 4, 6, 8, and 10) system is performed in the argon atmosphere to prevent oxidation. Both solutions of stoichiometric $SnCl_2$ (8.72 mmol) and alkylammonium chloride (17.44 mmol) are prepared using about 30 mL 2 M HCl solution at room temperature, separately. After mixing both solutions, the solution is kept for the reaction for 12 hours, and then cooled down from 90 °C to room temperature at a rate of 5 °C/h. The produced plate-like transparent crystals are dried under a vacuum for 48 hours and stored under argon atmosphere.

X-ray powder diffraction analyses are carried out with a philips 1710 diffractometer using Cu K_α radiation. A scan range of 5 to 80° and a scan step of 0.4° are used for the pattern recording. The EXAFS spectra at the Sn L_1-edge were measured in the transmission mode at room temperature using a standard setup of the BL3C1 at Pohang Light Source in the Pohang Accelerator Laboratory. The electron energy of the storage ring was 2.0 GeV and the synchrotron radiation was monochromatized using the Si (111) monochrometer. All of the infrared spectra are recorded from 1300 to 4000 cm^{-1} by using Bruker IFS66. The Raman spectra are recorded from 50 to 360 cm^{-1} on a 1 cm^{-1}/step by a Jasco NR-1100 model equipped with an argon laser. The 514.5 nm radiation for excitation is used with a power of 200 mW.

Calorimetric measurements are performed on a polymer laboratories DSC at a temperature range from room temperature to 200 °C with a heating rate of 5 °C/min. The powder sample is pressed into pellets with 3 ton/cm^2 pressure for PL measurements. PL measurements are also carried out by Kontron instruments SFM25 equipped with a Xenon lamp with an excitation wavelength of 480 nm.

Results and Discussion

X-ray diffraction. All crystallographic structures of the $(C_nH_{2n+1}NH_3)_2SnCl_4$ compounds are determined as an orthorhombic system at room temperature. The obtained XRD patterns are shown in Figure 2. The patterns show good solutions of layered compounds. The compounds consist of an $SnCl_4^{2-}$ infinite sheet of corner shared $SnCl_6$ octahedra by ionic bond, separated by bilayers of alkylammonium cations, with the ammonium group hydrogen and ionic bonding to halogens in the inorganic sheet. The relatively weak van der Waal's force between the alkyl chains separating the layers provides for a highly two-dimensional structure. The indexation is compatible with space group Pnma. Lattice parameter, reduced cell volume, and crystal systems are listed in Table 1. The lattice c parameter increases linearly with the n value. On the contrary, the lattice a and b values are almost invariable as shown in Figure 3. The length of alkyl chains significantly affects the distance between inorganic layers, and from the c-n graph's linearity, it can be considered that the organic

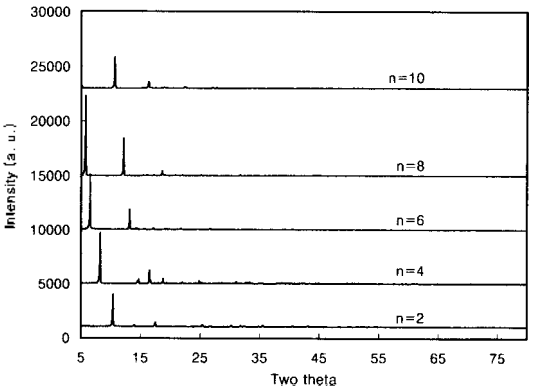

Figure 2. XRD patterns of $(C_nH_{2n+1}NH_3)_2SnCl_4$. The main peaks shift to larger d-value with the n increase.

Table 1. Lattice parameters, lattice volume, and crystal system for the $(C_nH_{2n+1}NH_3)_2SnCl_4$ compounds

	Lattice parameter (Å)			Cell volume (Å^3)	Crystal system
	a	b	c		
$(C_2H_5NH_3)_2SnCl_4$	7.785	7.610	25.21	1494	orthorhombic
$(C_4H_9NH_3)_2SnCl_4$	7.796	7.651	32.33	1928	orthorhombic
$(C_6H_{13}NH_3)_2SnCl_4$	7.840	7.670	40.90	2459	orthorhombic
$(C_8H_{17}NH_3)_2SnCl_4$	7.870	7.684	46.65	2821	orthorhombic
$(C_{10}H_{21}NH_3)_2SnCl_4$	7.931	7.751	53.21	3271	orthorhombic

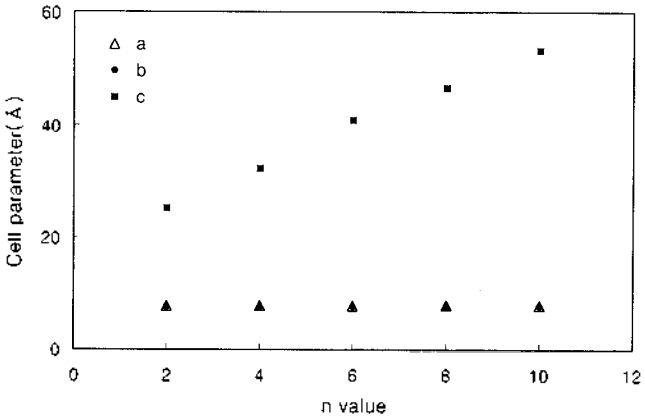

Figure 3. Variation of the lattice parameter a, b, c of orthorhombic $(C_nH_{2n+1}NH_3)_2SnCl_4$ system at room temperature with n value. The c parameter is increased linearly with n value increased, but a, b parameters is almost invariable with n value.

chains are mostly arranged in a same direction.

EXAFS spectroscopic analysis. EXAFS data were analyzed by using a nonlinear fitting method and computer code FEFF6 (University of Washington). From the result of the first shell EXAFS best-fit procedure, the local structures obtained from the $(C_nH_{2n+1}NH_3)_2SnCl_4$ system are shown in Figure 4. The quantum-well layer width of 5.26-5.74 Å is much smaller than the barrier layer widths which are about 7.35, 10.87, 15.09, 17.93, and 21.17 Å from the EXAFS spectra. The barrier layer widths are calculated using c/2 minus half of the octahedron widths in the c projection. It is a very good case of quantum-well materials due to the large different bandwidths between the insulating barrier and the conducting quantum-well layers. In $(C_nH_{2n+1}NH_3)_2$-$SnCl_4$, the Sn^{2+} is formally in a divalent state and therefore has a pair of nonbonding electrons in its outer electronic configuration. Typically, this lone pair of electrons results in a lowering of the coordination symmetry around these cations.[8] It is performed by EXAFS analyses. The stereochemical activity of the Sn(II) nonbonding electrons is apparent from the distorted octahedral coordination of chlorides, with two longer and two short Sn-Cl bonds in the a-b plane of the perovskite sheets.

FT-IR and Raman spectroscopy. The vibration spectra in the room temperature phase are studied in order to determine the structure of the alkylammonium chains. The wavenumbers of the observed vibration modes in the room temperature phase are listed in Table 2. The FT-IR spectra are almost the same in comparison to the n-alkylammonium salt. It means that the organic layer is not

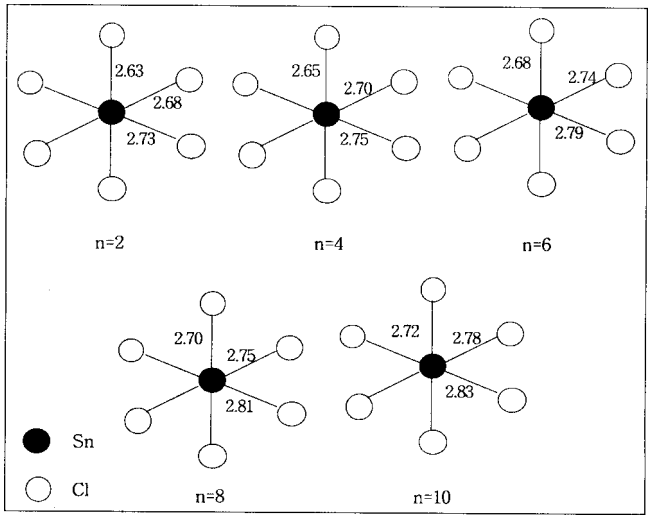

Figure 4. Local structure of the Sn-Cl bond with different bondlength along each direction.

Table 2. The vibration modes of FT-IR and Raman spectra for the $(C_nH_{2n+1}NH_3)_2SnCl_4$ system

Vibration mode		Wave numbers (cm^{-1})				
		n=2	n=4	n=6	n=8	n=10
FT-IR	stretch (N—H)	3210	3201	3203	3203	3201
	stretch (CH_3)(as.)	2982	2953	2951	2950	2950
	stretch (CH_2)(as.)	2934	2925	2918	2918	2918
	stretch (CH_2)(sy.)	2875	2865	2854	2849	2849
	NH_2 bending	1579	1576	1577	1576	1576
	CH_3, CH_2 bending	1473	1471	1472	1471	1471
	CH_3 bending(sy.)	1396	1384	1381	1380	1380
Raman	ν(Sn-Cl)	322	322	322	321	322
	LAM	244	246	246	246	249
	δ(Sn-Cl)	177	176	177	177	179

strongly coupled to the inorganic layer and keeps the RNH_3^+ ion state in the lattice. From the spectra as shown in Figure 5, red shifts have been found in all compounds as compared with the n-alkylammonium. Wave numbers of the N-H stretching mode and those of the N-H bending mode are shifted from 3300 to 3201 cm^{-1} and from 1600 to 1576 cm^{-1}, respectively, due to the interaction between the NH_3^+ polar head and axial chloride ion induced by the N-H force's constant reduction.

The Raman spectra show 3 peaks corresponding to the Sn-Cl stretching mode, the LAM (longitudinal acoustic mode), and the Sn-Cl bending mode[9] as shown in Figure 6. The line broadening takes place due to differences in the Sn-Cl bond-length.

DSC. The DSC curves observed in heating processes are shown in Figure 7. No phase transition takes place for the n=2 and 4. However, only one phase transition has been observed for the n=6 and 10 and two phase transitions for the n=8. Transition temperature, enthalpy change, and entropy change of $(C_nH_{2n+1}NH_3)_2SnCl_4$ compounds are listed in Table 3. The transition entropy change is computed from the relation of $\Delta S=\Delta H/T$. According to the magnitudes of ΔH and ΔS, the phase

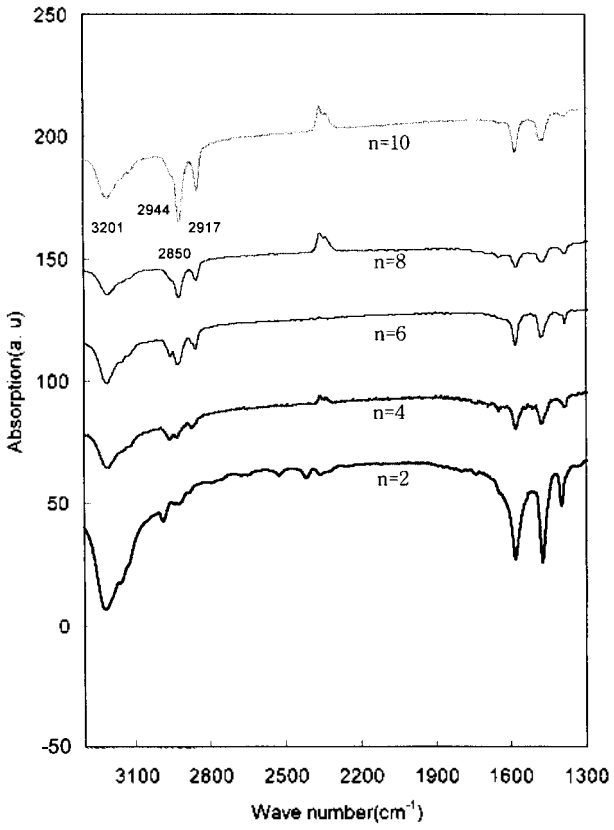

Figure 5. FT-IR spectra of the $(C_nH_{2n+1}NH_3)_2SnCl_4$ system.

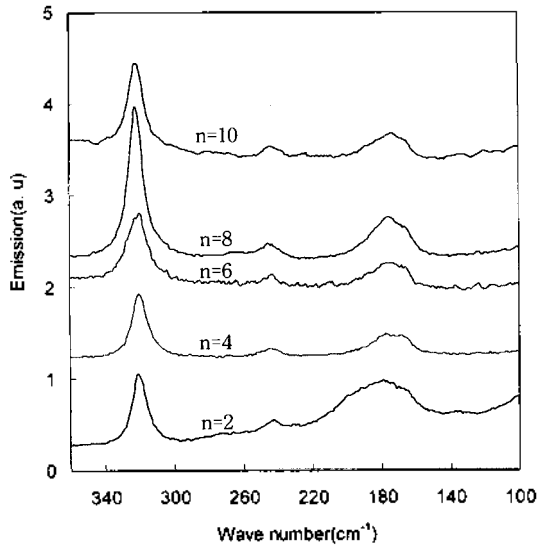

Figure 6. Raman spectra of the $(C_nH_{2n+1}NH_3)_2SnCl_4$ system.

transition concludes the partially melted phase transition. The ΔS value increases gradually as the carbon number increases, which means that the partial chain melting plays a dominant role in the major transition.[10] The phase transition temperature decreases with the increasing n value even though there is an increased van der Waal's interaction. The phase transition may represent not only the partial melting but also the $SnCl_4^{2-}$ layer change induced by NH_3^+ polar head reorientation. The partially melted phase transition is restricted by the inorganic frame

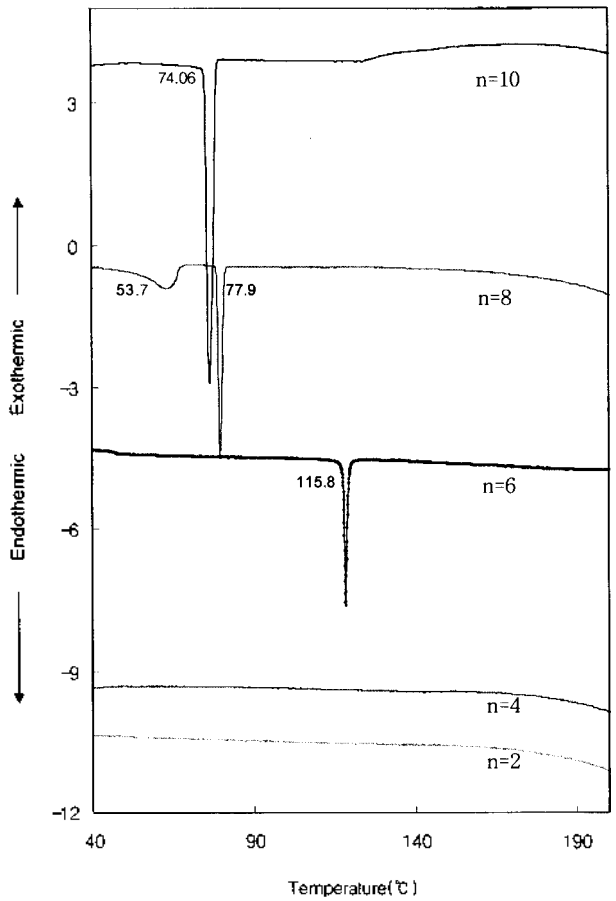

Figure 7. DSC patterns of the $(C_nH_{2n+1}NH_3)_2SnCl_4$ system.

Table 3. The phase transition temperature, enthalpy change, and entropy change of the $(C_nH_{2n+1}NH_3)_2SnCl_4$ system from the system DSC analysis

Compounds	T(°C)	ΔH (kJ mol^{-1})	ΔS (J mol^{-1}·K^{-1})
$(C_2H_5NH_3)_2SnCl_4$	—	—	—
$(C_4H_9NH_3)_2SnCl_4$	—	—	—
$(C_6H_{13}NH_3)_2SnCl_4$	115.8	1.11	2.85
$(C_8H_{17}NH_3)_2SnCl_4$	53.7	1.43	4.38
	77.9	1.91	5.44
$(C_{10}H_{21}NH_3)_2SnCl_4$	74.1	5.01	14.4

in the lattice which contacts more closely in the case of smaller n value, so the phase transition is not observed in the case of n=2 and 4. On the contrary, the larger n value compounds exhibit more instability and phase transitions at a lower temperature.

PL. The organic-inorganic compounds of the $(C_nH_{2n+1}NH_3)_2SnCl_4$ system form a natural quantum-well structure. The luminescence originates from electronic transitions within the inorganic perovskite layer rather than the organic layer. The simple organic layer is transparent in the visible spectra range. In the layered compounds of the $(C_nH_{2n+1}NH_3)_2SnCl_4$ system, the lowest exciton state arises from excitations between the valence band of the Sn(5s) state and the conduction band derived primarily from the Sn (5p) state. The photoluminescence spectra of $(C_6H_{13}NH_3)_2$-

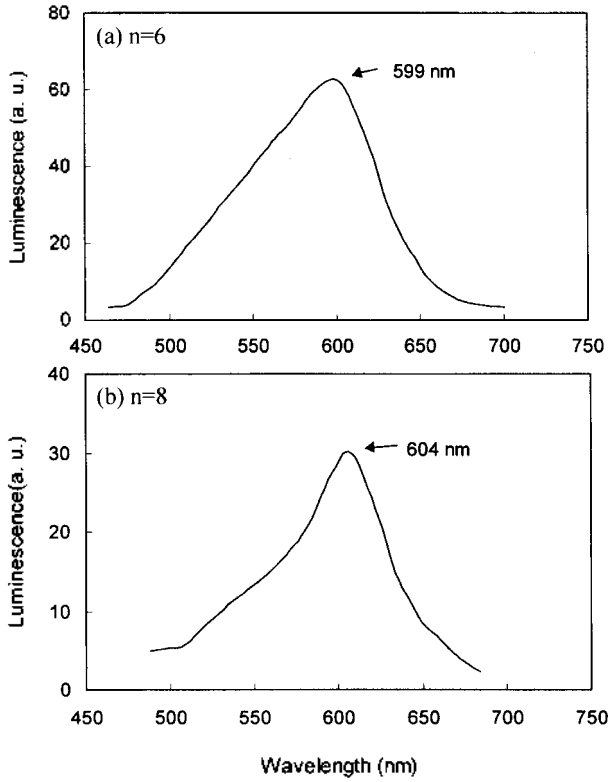

Figure 8. Photoluminescence spectra of the $(C_nH_{2n+1}NH_3)_2SnCl_4$ system at room temperature.

$SnCl_4$ and $(C_8H_{17}NH_3)_2SnCl_4$ are observed at 599 and 604 nm, respectively, as shown in Figure 8. The PL emission occurs from the bottom of the Sn(5p) band to the top of the Sn(5s) band, since the peaks appear at a similar position of wavelength in spite of differences of bond lengths for Sn-Cl.[11] In addition to the main spectral peak, they appear to decrease somewhat by exposure to air for several days, suggesting that this is a surface oxidation or degradation effect.

Conclusions

The quantum-well bilayer compounds of the $(C_nH_{2n+1}NH_3)_2$-$SnCl_4$ (n=2, 4, 6, 8, and 10) system have been synthesized by the low temperature solution technique. The natural quantum-well layered structure is identified by XRD, EXAFS, FT-IR, and Raman spectroscopic analyses. The bandwidth of Sn-Cl shows a different value along 3 axial directions. Phase transitions have been found in the compounds of n=6, 8, and 10 due to the partial melting of organic layers. The PL have been found at about 600 nm for the compounds of n=6 and 8.

Acknowledgment. The present study was supported by the Basic Science Research Institute Program, Ministry of Education of Korea, 1996, Project No. BSRI-96-3424. We are grateful to Dr. Jay Min Lee and authorities concerned of Pohang Light Source for their helps on the EXAFS measurement.

References

1. Ricard, L.; Rey-Lafon, M.; Biran, C. *J. Phys. Chem.* **1984**, *88*, 5614.
2. Ishihara, T. *J. of Luminescence* **1994**, *60&61*, 269.
3. Kitazawa, N. *Jpn. J. Appl. Phys.* **1996**, *35*, 6202.
4. Muljarov, E. A.; Tikhodeev, S. G.; Gippius, N. A.; Ishihara, T. *Phys. Rev. B*, **1995**, *51*, 20.
5. Guo, N.; Zeng, G.; Xi, S. *J. Phys. Chem. Solids* **1992**, *53*, 437.
6. Needham, G. F.; Willett, R. D.; Franzen, H. F. *J. Phys. Chem.* **1984**, *88*, 674.
7. Era, M.; Morimoto, S.; Tsutsui, T.; Saito, S. *Appl. Phys. Lett.* **1994**, *65*, 676.
8. David, B. Mitzi, *Chem. Mater.* **1996**, *8*, 791.
9. Elleuch, H.; Kamous, M.; Daoud, A.; Jouini, T. *Phys. Stat. Sol.* **1996**, *157*, 3.
10. Kang, J. K.; Choy J. H.; Rey-Lafon, M. *J. Phys. Chem. Solids.* **1993**, *54*, 1567.
11. Clark, S. J.; Flint, C. D.; Donaldson, J. D. *J. Phys. Chem. Solids.* **1981**, *42*, 133.